Elastic versus inelastic spin-polarized electron scattering from a ferromagnetic surface

Sergey N. Samarin,[1] Oleg M. Artamonov,[2] Alexander P. Baraban,[2] Mikhail Kostylev,[1] Paul Guagliardo,[3] Jamal Berakdar,[4] and James F. Williams[1]

[1]*School of Physics, University of Western Australia, Perth, Western Australia 6009, Australia*

[2]*Research Institute of Physics, St. Petersburg State University, St. Petersburg 199034, Russia*

[3]*Centre for Microscopy, Characterisation and Analysis, University of Western Australia, Perth, Western Australia 6009, Australia*

[4]*Institute of Physics, Martin Luther University of Halle-Wittenberg, Halle-Wittenberg, Halle 06120, Germany*

(Received 13 July 2016; revised manuscript received 18 September 2016; published 24 October 2016)

Spin-polarized electron energy loss spectroscopy was applied to study the intensity asymmetry upon the reversal of the incident spin polarization of elastically and inelastically scattered polarized electrons from an epitaxial ferromagnetic Fe layer on W(110). The polarization of the incident beam was always collinear with the magnetic moment (magnetization) of the sample, and the asymmetries were measured for two opposite magnetizations of the sample. They allowed extracting the exchange and the spin-orbit components from the measured asymmetry. A strong asymmetry of Stoner excitations in an Fe film on W(110) is observed, as expected, at about 3 eV energy loss. The value of the asymmetry declines but is still observable when the surface is contaminated. The asymmetry of elastic scattering for normal incidence and a 50° detection angle is close to zero in contrast to the Stoner excitation asymmetry (inelastic scattering). However, the asymmetry of elastic scattering increases substantially at two specular geometries with 25° and 72° angles of incidence, compared to the normal incidence, and may be even larger than the asymmetry of Stoner excitations. The sign of elastic scattering asymmetry changes upon the reversal of the sample magnetization, indicating the magnetic origin of this asymmetry, i.e., spin-dependent electron-electron scattering with electron exchange. The calculation of the asymmetry of elastic spin-polarized electron scattering from a spin-dependent surface potential barrier shows a qualitative agreement with the measurements.

DOI: 10.1103/PhysRevB.94.155440

I. INTRODUCTION

Spin-polarized electron energy loss spectroscopy (SPEELS) of ferromagnetic surfaces has a long and successful record as a method for investigating surface magnetism. The individual electron-hole excitations (Stoner excitations) [1–9] as well as collective (magnon) spin excitations [10–12] were studied using SPEELS. Fundamental aspects of the spin-orbit interaction (SOI) and the electron exchange can also be extracted from SPEELS [13,14]. SOI, on the other hand, is at the heart of currently discussed topics such as the quantum spin Hall effect [15–18], topological insulators (TI), graphene [19–21], and "spintronics" [22] in general. As a surface-sensitive probe, SPEELS can deliver important details of the spin-dependent scattering at interfaces and in layered structures.

The aim of the present work is a comparative analysis of the spin dependence of elastic and inelastic scattering of spin-polarized electrons from a ferromagnetic surface. A particular question is to what extent and under which conditions electron exchange effects (and exchange asymmetry) are present in elastic and inelastic scattering in the case of specular geometry, where the dipole scattering mechanism is expected to be dominant. The result of such an investigation is important to identifying the optimum geometric arrangement of SPEELS for a specific task, as well as for the adequate interpretation of SPEELS.

There are two spin-dependent effects that determine spin-related properties of surfaces and mediate electron scattering from surfaces: (i) electron exchange and (ii) spin-orbit interaction [23]. The first effect (exchange) is the consequence of the fermionic nature of electrons (spin-1/2 particles), and the Pauli exclusion principle. The second one results from the interaction of an electron spin with its orbital motion (momentum).

A well-known manifestation of the exchange effect is the Stoner excitation, involving electron-hole excitation with opposite spins for an electron and a hole, as observed in SPEELS of ferromagnetic samples [14].

The spin-orbit interaction shows up when spin-polarized electrons are scattered from the surface of high-Z materials such as tungsten, for example. In this case the scattering probabilities for the same spin are different for electrons scattered to the left and to the right. This leads to a left-right asymmetry of scattering of electrons upon reversal of the incident beam polarization. The same mechanism leads to the polarization of a scattered electron beam if it was unpolarized before scattering. The degree of polarization is defined as $P = (I^{+}–I^{-})/(I^{+} + I^{-})$, where I^{+} and I^{-} are the intensities of scattered electrons with spin projection parallel (I^{+}) or antiparallel (I^{-}) to the quantization axis. If the incident beam is spin-polarized (for simplicity, with 100% degree of polarization), then an intensity asymmetry of scattering is observed when we flip the polarization of the incident beam. This asymmetry we define as $A = (I^{\mathrm{up}}–I^{\mathrm{down}})/(I^{\mathrm{up}} + I^{\mathrm{down}})$, where I^{up} is the scattering probability (reflectivity) of incident electrons with spin-up and I^{down} is the scattering probability of incident electrons with spin-down. It turns out that $P = A$ in magnitude [23]. In other words, the surface, which can polarize an electron beam via scattering, can also work as a spin-dependent electron reflector i.e. as a spin detector (or as a spin-filter). Both of these effects can be described by spin-dependent reflection coefficients R^{up} and R^{down}, where the superscripts "up" and "down" refer to the polarization of the incident beam with spin orientation "up" or "down" respectively. If the

incident beam intensity is I_0 and the beam is partially polarized with polarization P_0, then the intensity can be decomposed into spin-up and spin-down intensities: ${I_0}^{\rm up} = (1 + P_0)I_0/2$, and ${I_0}^{\rm down} = (1–P_0)I_0/2$. The scattered intensities are given by $I^{\rm up} = R^{\rm up} \cdot {I_0}^{\rm up}$, and $I^{\rm down} = R^{\rm down} \cdot {I_0}^{\rm down}$. The asymmetry of scattering is then equal to $A = (R^{\rm up}–R^{\rm down})/(R^{\rm up} + R^{\rm down})$, which represents the intensity change upon the reversal of the incident beam polarization [24].

For a ferromagnetic surface, the reflection coefficients also depend on the direction of magnetization of the sample due to exchange. It means that there are now four spin-dependent reflection coefficients corresponding to four possible mutual orientations of the incident beam polarization and the sample magnetization: $R^{++}, R^{+-}, R^{-+}, R^{--}$, where the superscript "+" corresponds to "up", and "–" corresponds to the "down" orientation of the polarization vector of the incident electron beam or/and the majority spins in the ferromagnetic sample. If all four reflection coefficients are measured, then the exchange contribution to the asymmetry, spin-orbit contribution, and interference between exchange and spin-orbit contributions can be calculated as shown in [25].

II. EXPERIMENT

The experimental setup used in this work includes a spin-polarized electron source and a scattering chamber with a time-of-flight (TOF) electron energy analyzer [26] and facilities for sample preparation and characterization. The spin-polarized electron source and scattering chamber are separated by a vacuum valve allowing the two chambers to be evacuated and vented independently. The spin-polarized electron source is based on photoemission from a strained GaAs crystal (superlattice) activated by Cs deposition and oxygen adsorption [27]. Laser light with a wavelength of 835 nm passes through a linear polarizer and a liquid crystal retarder, which convert it to circularly polarized light. Photoelectrons excited from the activated GaAs crystal are longitudinally polarized. After passing through a 90° electrostatic spherical deflector, the electron beam becomes transversally polarized with the polarization vector "up" or "down," depending on the helicity of the laser light. The sign of the polarization of the electron beam can be changed by changing the helicity of the laser light, which is controlled by the liquid crystal retarder. To avoid artefacts in spin-dependent electron spectroscopy related to the changes of the sample surface conditions during the measurement (for example, surface contamination), the polarization of the incident beam was altered every 5 s and the data corresponding to each of the polarizations was stored in two files: spin-up and spin-down spectra. The TOF electron energy analysis is described in detail elsewhere [26]. The three geometric arrangements used in this work are depicted in Fig. 1. These geometries are chosen so as to allow comparing the spectra measured at normal incidence and at specular geometry. In addition, two specular geometries were chosen with very different angles of incidence. The particular angles (50° and 144°) are dictated by constraint due to the experimental vacuum chamber and the flanges available for detectors.

The iron films were deposited on the W(110) surface using an OMICRON-type evaporator (EFM-3). The substrate [tungsten crystal (110) face] was cleaned prior to the film deposition using routine cleaning procedures, including oxygen treatment and high-temperature flashes [28,29]. The thickness of the film was estimated using a quartz microbalance and Auger electron spectroscopy. An integrated low-energy electron diffraction (LEED)-Auger system (SPECS) was used to control the cleanliness and crystal structure of the substrate and deposited films. The base pressure in the experimental chamber was in the 10^{-11} Torr range. The W(110) crystal substrate was mounted on a twofold rotatable manipulator that allowed a sample rotation around both the vertical (polar angle θ) and horizontal (azimuthal angle ϕ) axes. The $[1\bar{1}0]$ direction along the surface of the tungsten crystal was identified and the azimuthal position of the sample corresponds to $\phi = 0$ when this crystallographic axis runs along the vertical rotational axis and perpendicular to the scattering plane. Magnetic anisotropy of the iron film on W(110) drives the magnetization of the film (in the thickness range below 100 Å) along the $[1\bar{1}0]$ direction of the substrate parallel to the film surface.

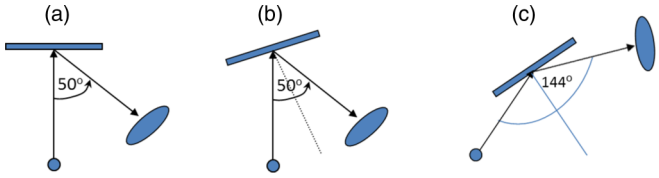

FIG. 1. Three geometrical arrangements used in this work.

III. EXPERIMENTAL RESULTS

The three geometrical arrangements shown in Fig. 1 were used to measure SPEELS of a thin ferromagnetic layer (Fe) on W(110) with low-energy spin-polarized incident electrons. All spectra were measured for four mutual orientations of the polarization vector of the incident electron beam and magnetic moment of the ferromagnetic film. The magnetic moment of the sample was oriented first downwards (the majority spins of the sample point upwards in this case), and then the magnetic moment was flipped down. Both vectors, the polarization vector of the beam and the magnetization direction of the sample, are perpendicular to the scattering plane and were chosen to be parallel or antiparallel to each other. For each orientation of the sample magnetic moment (M1 and M2), the energy distributions of the scattered electrons were measured for the spin-up ($I^{\rm up}$) and the spin-down ($I^{\rm down}$) polarizations of the incident beam, and the corresponding asymmetries were calculated as $A_{\rm M1} = (I^{\rm upM1}–I^{\rm downM1})/(I^{\rm upM1} + I^{\rm downM1})$ and $A_{\rm M2} = (I^{\rm upM2}–I^{\rm downM2})/(I^{\rm upM2} + I^{\rm downM2})$. Then, to leading terms (neglecting interference between exchange and spin-orbit scattering amplitudes), the spin-orbit and exchange contributions to the measured asymmetry are [14]

$$A_{\rm ex} = {}^1\!/_2(A_{\rm M1}–A_{\rm M2}),$$

$$A_{\rm SO} = {}^1\!/_2(A_{\rm M1} + A_{\rm M2}).$$

Figure 2(a) shows asymmetries of SPEELS measured for two opposite magnetizations of the sample M1 and M2, and for two different geometrical arrangements: (i) at normal incidence and detection at 50°, and (ii) specular geometry with an incidence angle (and detection angle) of 25°. For the

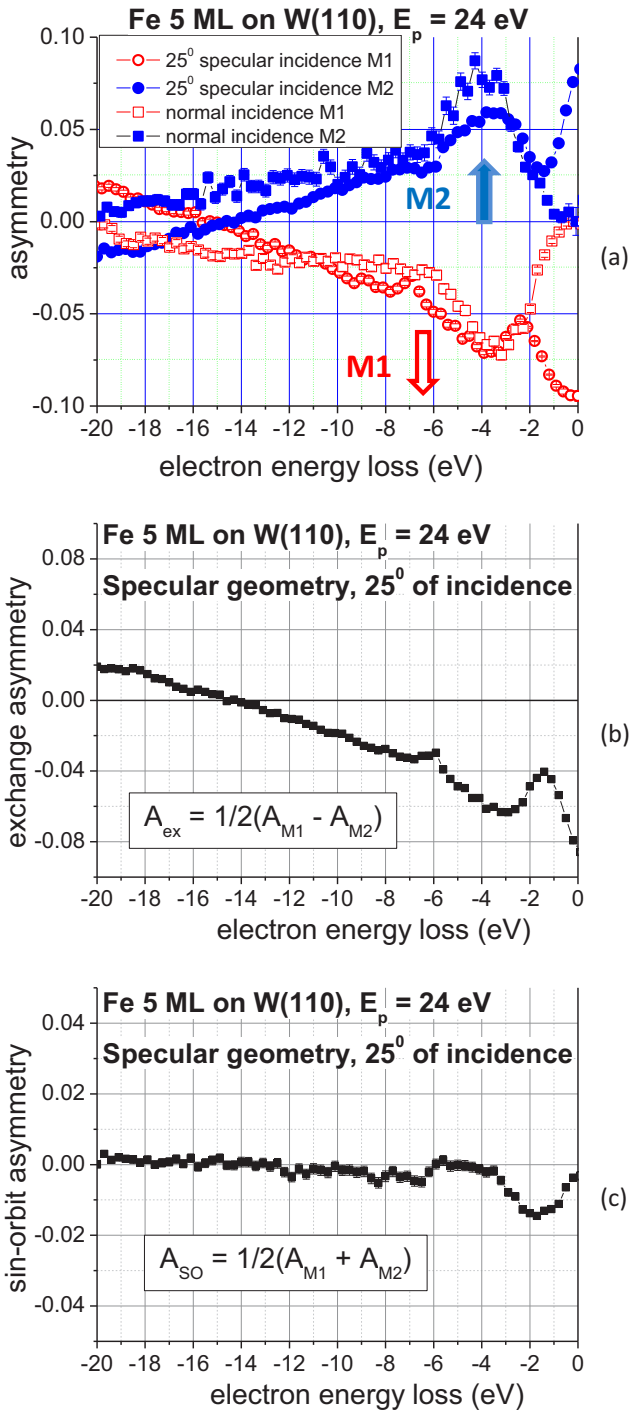

FIG. 2. (a) Asymmetry of SPEELS for two geometries and two magnetizations of the sample, (b) exchange component of asymmetry, and (c) spin-orbit component of asymmetry.

magnetization M1, asymmetry minima at about 3.5 eV and 7 eV energy losses correspond to the Stoner excitations, where an electron-hole pair with opposite spin characters is excited [14].

The asymmetry changes sign when the magnetization of the sample is reversed, confirming the magnetic origin of the asymmetry. For both of the above-mentioned geometries, the magnitude of this asymmetry is the same with the energy position being slightly changed. However, the most striking result is that for the normal incidence the amplitude of the elastic maximum in the spectrum is the same for both polarizations of the incident beam, i.e., the intensity asymmetry is equal to zero, whereas for the specular geometry the asymmetry of elastic scattering is quite large and reaches 9% (for M1).

For the specular geometry both the elastic and inelastic intensity asymmetries almost perfectly flip around the x axis when the magnetization of the sample reverses, indicating that the dominant contribution is the exchange effect in the measured asymmetry. For this geometry the exchange and the spin-orbit components of the asymmetry were determined following [14] and are shown in Figs. 2(b) and 2(c), respectively. In the exchange component [Fig. 2(b)] the Stoner excitation asymmetry is clearly visible at about 3 eV and 7 eV, and the asymmetry of elastic scattering at zero energy loss is -8%. It is somewhat surprising that the asymmetry of elastic scattering has a dominant contribution from exchange asymmetry (8%) and almost no spin-orbit contribution. The spin-orbit component of asymmetry [Fig. 2(c)] is zero at all energies except 2-eV energy loss, where it reaches value of -1.5%. The origin of this feature is not explained so far.

When SPEELS spectra were measured on the Fe film, which was exposed to the residual gas in the vacuum chamber (mostly CO and H_2) with the pressure in the 10^{-11} Torr range for 4 weeks, the asymmetries in the spectra change (Fig. 3). Figure 3(a) shows asymmetry of SPEELS measured on the contaminated 5-monolayer (ML) Fe film at two geometries and two magnetizations of the film. The magnitude of the asymmetries declines as compared to the clean Fe film, and the energy position of the Stoner excitation asymmetry is moved to about 2 eV for specular geometry, whereas for the normal incidence it is still at 3.5 eV. The exchange and the spin-orbit components of the asymmetry are shown in Figs. 3(b) and 3(c), respectively. The exchange component is just reduced in magnitude, whereas the spin-orbit component changed substantially: the feature in the asymmetry spectrum at 2-eV energy loss disappeared, but in the elastic scattering the spin-orbit component appeared.

Much larger changes in the asymmetry of SPEELS occur when the incidence angle in the specular geometry increases up to 72°. Figure 4 shows intensity asymmetry spectra measured on a 5-ML Fe film on W(110) at two specular geometries: with 25° and 72° angles of incidence. One can see that not only does the shape and magnitude of the asymmetry change but that the sign also changes. For the specular geometry with a 25° angle of incidence, there is a clear structure in the asymmetry spectrum of energy losses from 2 eV down to 8 eV, which is related to Stoner excitations.

The magnitude of the asymmetry reaches a value of 5%. In contrast, for the specular geometry with the 72° incident angle, the dominant feature in the asymmetry spectrum is the elastic maximum, with the asymmetry value reaching 17% (for magnetization M1) and no structure in the region of energy losses. The exchange and the spin-orbit contributions to the measured asymmetry (for the 72° angle of incidence) are presented in Fig. 5. It is seen that the exchange component of the asymmetry of the elastic scattering reaches up to 15%, whereas the maximum of the spin-orbit component of asymmetry of

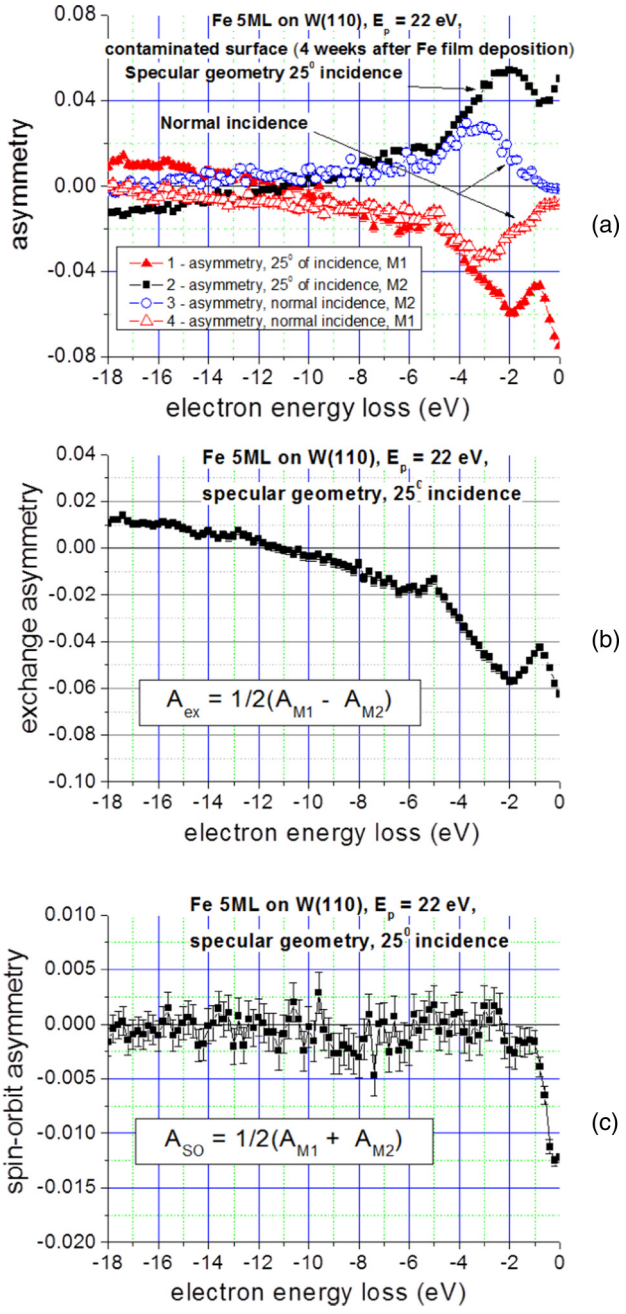

FIG. 3. The same as in Fig. 2, but for the contaminated surface of Fe film.

elastic scattering is only 4%. For a specular geometry, when the angle of incidence becomes larger, the exchange asymmetry of elastic scattering in SPEELS increases. To obtain some insight into this tendency, the asymmetry of SPEELS was measured on an ultrathin (2-ML) layer of Fe at specular geometry and 72° angle of incidence. The asymmetry spectrum is compared with the spectrum of the substrate. These results are presented in Fig. 6. In the SPEELS spectra [Figs. 6(a) and 6(b)], one can immediately see that the deposition of 2 ML of Fe changes the intensities of the elastic maxima for spin-up and spin-down primary electrons, i.e., it leads to the intensity asymmetry of elastic scattering. Indeed, on Fig. 6(c) the asymmetry of elastic scattering from the surface with 2 ML of Fe is about 8%, whereas for the clean W(110) substrate this asymmetry is close to zero. At the same time, the asymmetry structure in the energy-loss region of the spectrum between 10 and 16 eV is clearly observable in the spectrum of the W substrate, as well as in the spectrum of the ultrathin iron layer on W(110). This observation indicates that the origin of the asymmetry in the inelastic part of the spectrum is the spin-dependent electron scattering from the W(110) surface or from the Fe/W interface. It also shows that the incident electrons penetrate through the Fe layer and undergo scattering from the W surface (more precisely, from Fe/W interface). The deposition of a very thin layer of Fe (2 ML) changes the asymmetry in elastic scattering dramatically. It is instructive to compare this asymmetry spectrum with the spectrum of a thicker Fe film, for the same geometry and primary electron energy (see Fig. 5). At a film thickness of 5 ML there is no contribution from the substrate. The main outcomes of these results are:

(i) For a specular geometry with both 25° and 72° angles of incidence, the intensity asymmetry of elastic scattering of spin-polarized electrons increases compared to normal incidence, and

(ii) The asymmetry in Stoner excitations depends on the scattering geometry, and does not disappear at the specular geometry, in general, but becomes invisible for particular geometries and primary electron energies (for example, at specular geometry, 72° of incidence and 20 eV primary energy). Since the dependence of the Stoner excitation asymmetry on the kinematics of scattering was discussed earlier [30], we will focus mostly on the asymmetry of elastic scattering of spin-polarized electrons from the ferromagnetic surface.

IV. DISCUSSION

The reasons for the dependence of elastic scattering from a ferromagnetic surface on the spin orientation of the incident electron beam have been thoroughly analyzed in [31], with the following conclusions:

(i) **Spin-orbit interaction**, which is weak for low-Z ferromagnetic materials (like Fe, for example) and can be excluded by the choice of the scattering geometry: if the polarization vector of the incident beam is in the scattering plane the spin-orbit contribution to the intensity asymmetry is zero;

(ii) **Dipole-dipole interaction** between the incident electron and the magnetic ground-state electrons of the target, which depends on the mutual orientation of the incident electron spin and the magnetic moment of the target; the dipole-dipole term is very small for $E \ll mc^2$ and can be neglected for low (below 100 eV) primary electron energies;

(iii) Since the spin-orbit interaction is neglected for low-Z metals (Fe), **the exchange interaction** becomes the main driving force of spin dependence in elastic scattering and the scattering of polarized electrons from Fe can be described by the Pauli equation. The effective magnetic field in the Pauli equation can be expressed as $\mathbf{B}_{\text{eff}} = \Delta V_{\text{ex}} \times \mathbf{m}$, where $\mathbf{m}$ is the unit vector in the direction of the majority spin axis and ΔV_{ex} is the spin-dependent deviation from the averaged exchange potential: $V_{\text{ex}} : V_{\text{ex}}{}^{\uparrow\downarrow} = V_{\text{ex}} \pm \Delta V_{\text{ex}}$, where the arrows indicate the potential for spin-up and spin-down electrons. The main problem is to choose a realistic spin-dependent effective potential $V_{\text{ex}}{}^{\uparrow\downarrow}$. As is usual in LEED theory, it should contain

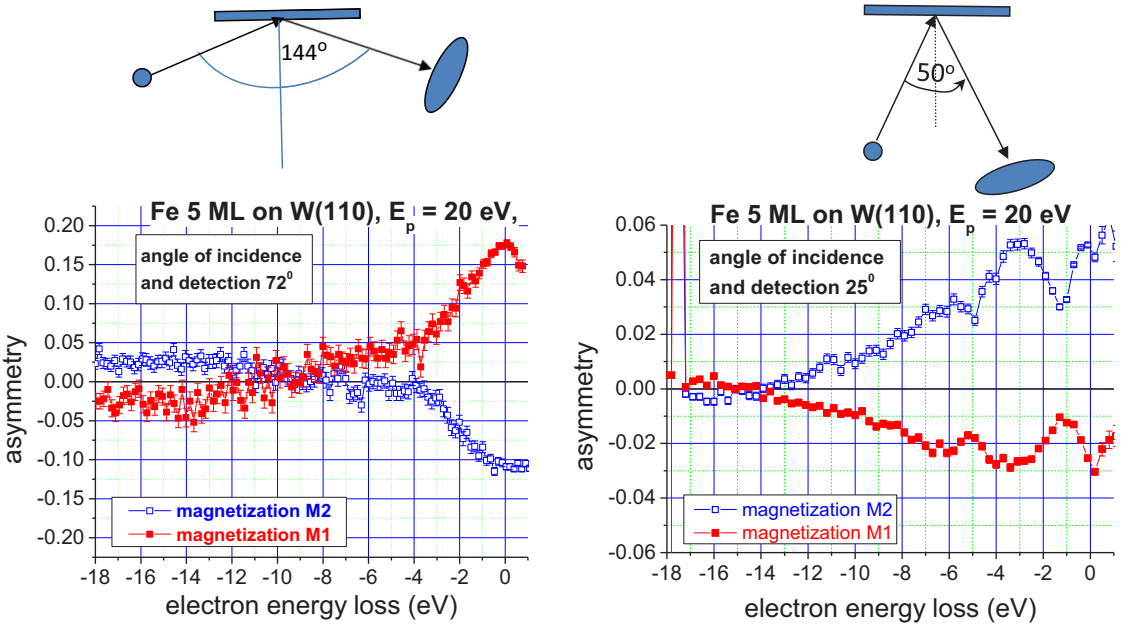

FIG. 4. Intensity asymmetry of SPEELS at specular geometry with 72° (left) and 25° (right) of incidence.

real and imaginary parts, both of which are spin dependent. The real part is spin-dependent due to the exchange interaction of the incident electron with majority and minority electrons of the sample (it is energy dependent). The imaginary part of the potential, which is responsible for the absorption and energy losses, receives its spin dependence from the spin-dependent energy-loss channels. These channels may include in general: phonon excitation, magnon excitation, single-electron excitations (interband transitions), and plasmon excitation. It was shown (Ref. [31] and references therein) that the contributions from electron-hole excitation (V_{eh}) and plasmon excitation (V_p) are an order of magnitude larger than the contributions to the imaginary part of the scattering potential from magnon and phonon excitations. However, the plasmon excitation should be at most very weakly spin dependent because it involves simultaneously majority and minority electrons of the valence band. As for electron-hole excitation, the heuristic model of spin-dependent potentials $V_{eh}{}^{\uparrow\downarrow}$ involves two suppositions:

(a) Isotropic electron-electron scattering at low energies (a few electronvolts). Consequently, the scattering amplitude for two electrons with parallel spins (triplet scattering), $f(\theta)$ - $f(\pi$ - $\theta)$, vanishes, i.e., scattering takes place only between electrons with opposite spin orientation (singlet-scattering-only hypothesis). However, the ratios between scattering probabilities for incident electrons with spin-up and spin-down are not determined.

(b) The second hypothesis suggests that the ratio $V_{eh}{}^{\uparrow}/V_{eh}{}^{\downarrow}$ should be given by the ratio of the respective scattering partners: $V_{eh}{}^{\uparrow}/V_{eh}{}^{\downarrow} = n^{\downarrow}/n^{\uparrow}$, where $n^{\downarrow}(n^{\uparrow})$ is the number of the spin-down (spin-up) electrons of the valence band (per atom). Then the total imaginary potential is $V_{im}^{\uparrow\downarrow} = V_{eh}^{\uparrow\downarrow} + V_p$.

(iv) **The spin-dependent surface potential barrier plays an important role in elastic scattering** of low-energy spin-polarized electrons from surfaces; it is a necessary ingredient for the observation of a fine structure in very low-energy

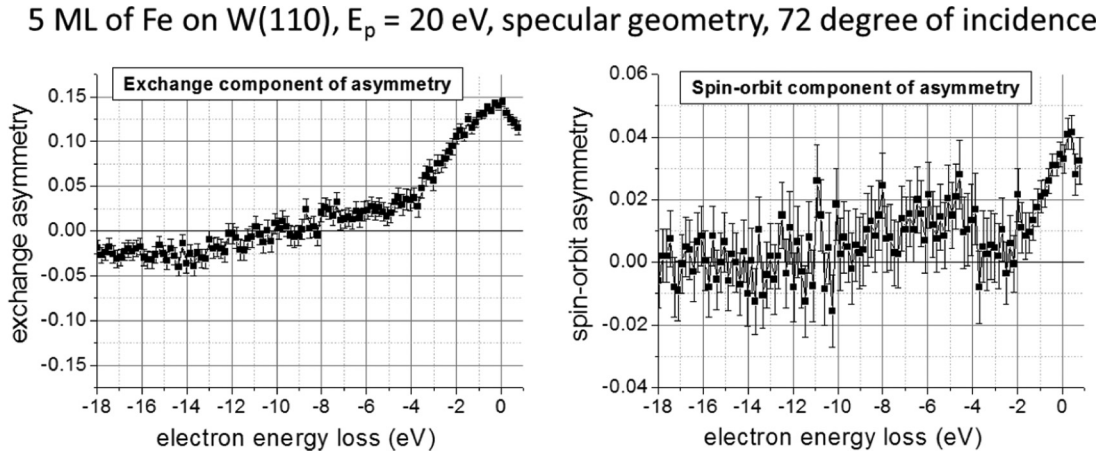

FIG. 5. Exchange and spin-orbit components of asymmetry.

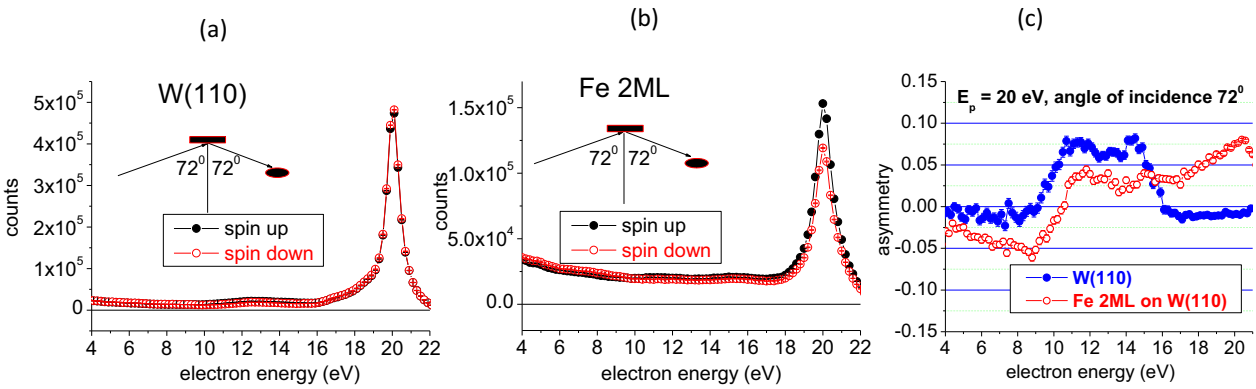

FIG. 6. (a) SPEELS spectra of W(110), (b) SPEELS of 2 ML of Fe on W(110), and (c) asymmetry of SPEELS for (a) and (b).

electron diffraction (VLEED) experiments [32,33]. The general shape of the surface barrier can be derived from two basic assumptions [34]. First, the electric charge located at a distance Z from the metal surface at Z_0, which is also referred to as the "mirror image plane," generates an "image charge" inside the metal mirror symmetric to the incident charge. Therefore the electrical potential experienced by the charge has a Coulomb-like shape: $V(z) = 1/[2(z-z_0)]$ for $z < z_0$ (atomic units are used) [Fig. 7(a)]. This shape of the potential is proven to be acceptable far outside of the solid, i.e., for $Z \ll Z_0$. The second assumption is, inside a free-electron metal, a constant "inner" potential V_{inner} is assumed. The transition between these two regions can be described by various models and approximations and was

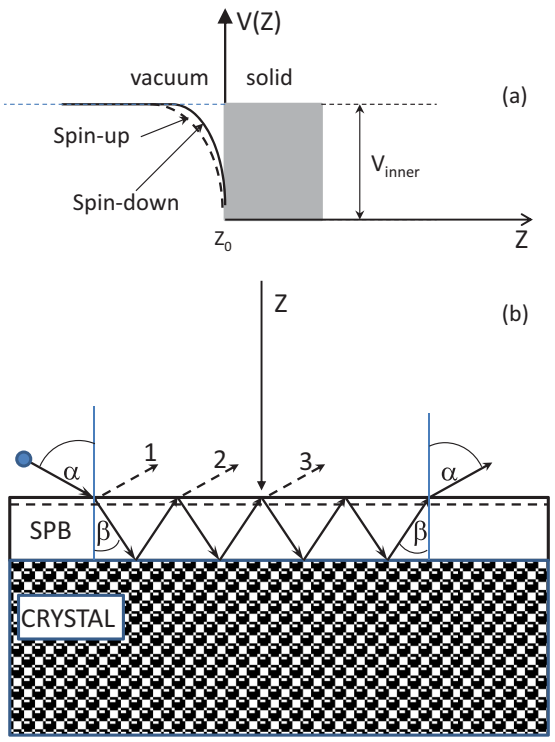

FIG. 7. Spin-dependent surface potential barrier (SPB) (a), and combined electron scattering from the surface barrier and the crystal surface (b).

discussed in detail in [35–37]. Qualitatively, the shape of the surface potential barrier depends on the rearrangement of the valence electrons near the Fermi level caused by the incident electrons. Since the density of states in a ferromagnetic sample is different for spin-up and spin-down electrons, incident electrons with different spin orientation interact differently with the electronic system of the sample due to electron exchange. This may lead to the spin dependence in the surface potential barrier. In fact, such a dependence was predicted theoretically [38,39] and observed experimentally using the inverse photoemission technique [40,41]. The presence of the surface potential barrier makes electron scattering from surfaces more complicated and requires the consideration of the scattering of incident electrons, not only by the crystal itself, but also by the surface barrier. In brief, scattering from a crystal surface involves diffraction because of the periodic arrangement of atoms along the surface: an incident electron wave with the wave vector $\mathbf{k}_0$ is scattered by surface atoms and then scattered waves interfere, giving rise to diffracted beams with wave vectors $\mathbf{k}_n$. The components of wave vectors parallel to the surface are determined by the Laue diffraction condition: $\mathbf{k}_{0||}-\mathbf{k}_{n||} = n\mathbf{g}$, where $\mathbf{g}$ is a reciprocal lattice vector of the two-dimensional surface lattice and n is an integer. In contrast to the scattering by crystal, scattering by the surface potential barrier (which can be considered as a one-dimensional potential) does not involve diffraction and $\mathbf{k}_{||}$ never changes. Scattering of an incoming plane wave by such a barrier (one-dimensional potential) is usually described by four complex scattering coefficients: r^{-+},r^{+-},t^{++},t^{--}, where superscripts indicate electron motion relative to the Z-axis direction. The coefficients r^{+-} and r^{-+} transform the amplitudes of incident waves into amplitudes of reflected waves, and t^{++} and t^{--} transform incident wave amplitudes into transmitted wave amplitudes. These coefficients depend on the model of the barrier (shape of the barrier) and can only be calculated numerically. A detailed description of how this can be done for various barrier models is given in [42].

It was demonstrated theoretically that the intensities of electron reflection from a realistic barrier alone do not show oscillatory behavior, as long as the crystal reflection is neglected. On the other hand, LEED calculations that disregard scattering from the surface barrier show no fine structure [43]. This means that the fine structure in VLEED is

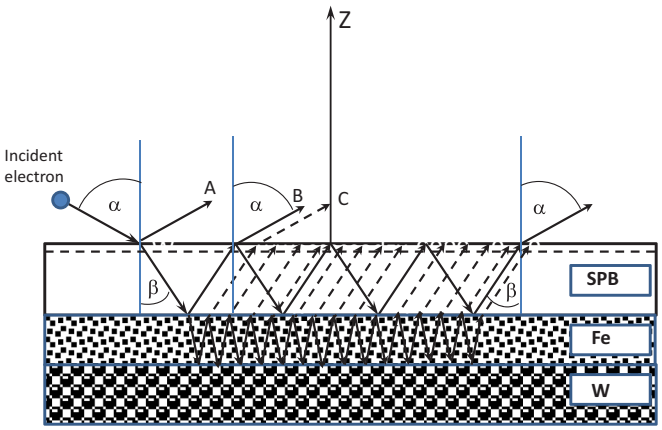

FIG. 8. Schematic representation of a surface with surface potential barrier (SPB), ultrathin layer (Fe) deposited on a substrate (W).

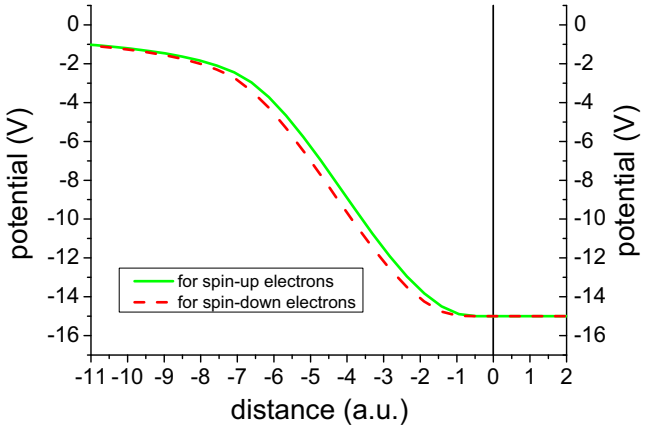

FIG. 9. Spin-dependent SPB. x axis is directed along the normal to the sample surface; the vertical axis represents the value of the potential. On the positive segment of the x axis the potential assumes a constant value of -15 V inside the metal, the negative segment of the x axis is in a vacuum, and the potential asymptotically tends to zero (vacuum level) at infinity. The potential for the majority electrons (spin-up) is shown as a solid line and for the minority electrons (spin-down) a dashed line.

caused by the interference between the crystal and the surface barrier scattering. There are few elastic scattering processes that contribute to the specular backscattered amplitude: (i) direct scattering from the barrier (dashed arrow 1 in Fig. 7); (ii) transmission through the barrier and backscattering from the crystal and then transmission through the barrier into the vacuum (dashed arrow 2 in Fig. 7); (iii) electrons scattered from the crystal can be scattered back from the surface barrier, scattered a second time from the crystal; after that it is transmitted through the surface barrier into the vacuum (dashed arrow 3 in Fig. 7). This bouncing of the electron wave between the crystal surface and the surface barrier may take place many times before it escapes from the surface.

The reflection and the transmission of the electron beam at the barrier and the crystal are determined by the coefficients: r^{+-},r^{-+},t^{--},t^{++}, R. The beams escaping from the surface are summed up with corresponding phases and form a total scattering amplitude. Depending on the phase shift they may lead to constructive or destructive interference. In the case of a spin-polarized incident beam, the surface potential barrier described above depends on the spin orientation of the incident beam relative to the magnetization of the sample surface [see Fig. 7(b)]; the surface barriers for two spin orientations of the incident beam are indicated by the solid and dashed lines in Fig. 7. Now all transmission and reflection coefficients become spin-dependent. Consequently, total scattering amplitudes for spin-up and spin-down electrons can be different; hence the intensity asymmetry can appear in spin-polarized electron scattering due to the surface potential barrier (SPB).

The situation becomes more complicated when an ultrathin ferromagnetic layer (for example, Fe) is deposited on a substrate [W(110) in our case]. Then the surface can be schematically represented as in Fig. 8. Now, there are three interfaces where electrons are scattered. At each interface electrons can scatter back or transmit into adjacent media. In Fig. 8 three scattering paths are shown and denoted by (A), (B), and (C). The first one (A) is the direct scattering from the SPB. The second one, (B), results from the scattering at the SPB and the surface of the ultrathin layer. The third one (C) involves scattering (and transmission) at three surfaces including the Fe/W interface. In the second and third paths the electron wave can bounce between two surfaces several times before coming out of the surface. All three beams, A, B, and C, can then undergo constructive or destructive interference depending on their relative phase difference, thus resulting in an increase or decrease of the scattered electron intensity. Given that the electron reflection and transmission at each surface is spin-dependent (at the SPB the solid and dashed lines indicate the barrier position for spin-up and spin-down incident electrons), the resulting scattering intensities for spin-up and spin-down incident electrons may be different. Thus, an intensity asymmetry can be observed. It is important to note that the intensity variation of elastic electron scattering as a function of primary energy (known as a fine structure in VLEED) results from the interference of scattering amplitudes. The intensity asymmetry, on the other hand, results from the spin dependence of elastic scattering of electron waves at interfaces and the surface potential barrier.

To check the possible influence of a spin-dependent surface potential barrier on the asymmetry of elastic spin-polarized electron scattering from a ferromagnetic surface, we performed calculations of the specular reflection coefficients for spin-up and spin-down incident electrons using a realistic shape of the SPB.

For a description of the potential barrier on the surface of Fe (110) the parameterized dependence from [34] is used. The shapes of the barrier for two spin orientations of the incident electrons are shown in Fig. 9. The solid line represents the barrier for the majority (spin-up) electrons and the dashed line for the minority (spin-down) electrons.

The specular reflection coefficients for spin-up and spin-down electrons from the surface potential barrier were calculated using the approach of [44]. The underlying physics of these calculations is described in [37]. It was shown there that at energies less than 30–40 eV it is important to take into account not only the refraction of the electron trajectories

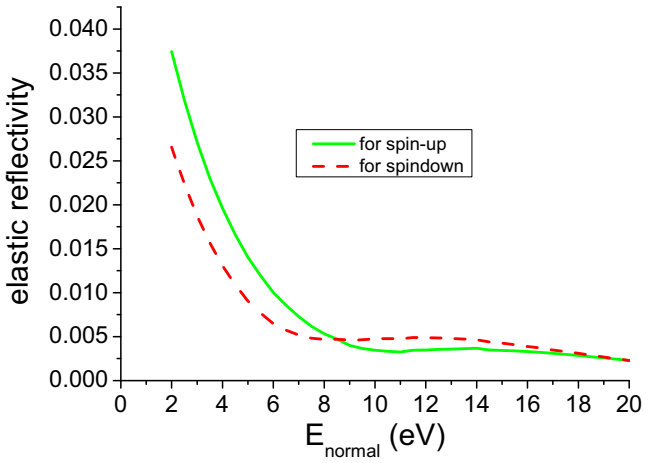

FIG. 10. Dependence of the specular reflection coefficients on the normal component of the electron kinetic energy E_{normal} for spin-up (solid line) and spin-down (dashed line) electrons from the potential barrier of Fig. 9.

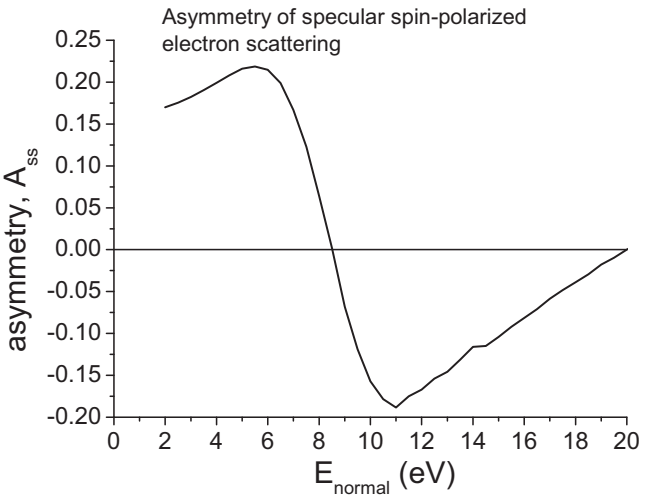

FIG. 11. Energy dependence of the spin asymmetry of the specular reflection of electrons from the Fe(110) surface potential barrier. It depends on the normal component of the electron kinetic energy E_{normal}.

at the potential barrier, but also the reflection of electrons from the barrier. It was pointed out that the electron reflection from the potential barrier depends very much on the shape of the barrier and on the normal to the surface component of the electron energy. This component of the electron kinetic energy is associated with the normal to the surface component of the electron momentum and is determined by the energy and the angle of incidence. Specular reflection coefficients as a function of the normal component of the electron kinetic energy for the majority (spin-up) electrons and for the minority (spin-down) electrons are shown in Fig. 10 by the solid line and by the dashed line, respectively.

Starting from Fig. 10 one can calculate the spin asymmetry of specular reflection of electrons as $A_{\text{ss}} = (R\uparrow - R\downarrow)/(R\uparrow + R\downarrow)$, where the arrows indicate the reflection coefficients for majority and minority electrons from the potential barrier. The asymmetry as a function of the normal to the surface component of energy is shown in Fig. 11.

At the electron energy of 20 eV and angles of incidence of 25° and 72° the normal to the surface components of energy are 16.4 eV and 1.9 eV, respectively. Spin asymmetry for the specular reflection of electrons at these angles of incidence is found to be −0.072 and 0.169, respectively. This means the asymmetry changes the sign, when the incident angle changes from 25° to 72°. In Fig. 4, where the SPEELS spectra for this primary electron energy (20 eV) and these angles of incidence (25° and 72°) are shown, one can see that the asymmetry of elastic electron scattering indeed changes the sign when the angle of incidence changes from 25° to 72°. The magnitudes of the asymmetries are of the same order as the calculated values. Another experimental result that might be due to the formation of the spin-dependent surface potential barrier is the increase of the asymmetry of elastic electron scattering after the deposition of a thin Fe layer on W(110), which is shown in Fig. 6. Indeed, the normal to the surface component of the electron energy in this case is about 2 eV, which corresponds to a substantial asymmetry of the elastic electron scattering from a spin-dependent potential barrier (see Fig. 11).

Thus, the theoretical estimate of the spin asymmetry of elastic electron scattering and its comparison with the experimental results indicate that the spin-dependent surface potential barrier may indeed be the cause for this asymmetry. A strong dependence of the asymmetry on the parameters of the surface potential barrier can be used to study the details of the barrier.

V. CONCLUSION

SPEELS spectra excited by low-energy (20–24 eV) spin-polarized electrons from thin ferromagnetic layers of Fe on W(110) were recorded at normal incidence (detection at 50°) and specular geometries with 25° and 72° angles of incidence. At specular geometry, for both 25° and 72° angles of incidence, the intensity asymmetry of elastic scattering of spin-polarized electrons increases compared to normal incidence, and this asymmetry is mostly due to the exchange effect. Given that the sample is an epitaxial (crystal) layer of Fe, the specular geometry of the electron scattering corresponds to the detection of the (00) diffracted beam. In this case a coherent (and multiple) scattering of polarized electrons on a spin-dependent potential barrier may lead to the intensity asymmetry. The intensity asymmetry of inelastic scattering (Stoner excitations) also depends on the kinematics of the scattering. It does not disappear, in general, for a specular geometry but becomes invisible at a particular geometry and primary electron energy (for example, at specular geometry, 72° of incidence, and 20 eV primary energy). The role of spin-dependent electron scattering at the surface potential barrier and interfaces is qualitatively discussed. Calculations of the asymmetry of elastic electron scattering from a spin-dependent surface potential barrier show a fair agreement with the experiment. Systematic measurements of the angular and primary energy (low-energy range 10–30 eV) dependence of the elastic and inelastic scattering in SPEELS from ferromagnetic surfaces will be carried out in the future. They will elucidate the mechanisms of such scattering and empower the analytical capabilities of SPEELS.

ACKNOWLEDGMENTS

This research was supported by the Australian Research Council and the University of Western Australia. We are grateful to J. Kirschner and F. O. Schumann for fruitful discussions. O.M.A. acknowledges Saint-Petersburg State University for Research Grant No. 11.38.187.2014. We thank S. Key and G. Light (UWA) for their technical support.

[1] H. Hopster, R. Raue, and R. Clauberg, Phys. Rev. Lett. **53**, 695 (1984).
[2] J. Kirschner, Phys. Rev. Lett. **55**, 973 (1985).
[3] J. Kirschner and S. Suga, Surf. Sci. **178**, 327 (1986).
[4] H. Hopster, D. L. Abraham, and D. P. Pappas, J. Electron Spectrosc. Relat. Phenom. **51**, 301 (1990).
[5] S. Modesti, F. Dellavalle, R. Rosei, E. Tosatti, and J. Glazer, Phys. Rev. B **31**, 5471 (1985).
[6] H. J. Hopster, J. Appl. Phys. **57**, 3017 (1985).
[7] J. Kirschner, Surf. Sci. **162**, 83 (1985).
[8] D. Venus and J. Kirschner, Phys. Rev. B **37**, 2199 (1988).
[9] J. Kirschner and S. Suga, Solid State Commun. **64**, 997 (1987).
[10] R. Vollmer, M. Etzkorn, P. S. Anil Kumar, H. Ibach, and J. Kirschner, Phys. Rev. Lett. **91**, 147201-1 (2003).
[11] G. Vignale and K. S. Singwi, Phys. Rev. B **32**, 2824 (1985).
[12] J. Prokop, W. X. Tang, Y. Zhang, I. Tudosa, T. R. F. Peixoto, Kh. Zakeri, and J. Kirschner, Phys. Rev. Lett. **102**, 177206 (2009).
[13] *Polarized Electrons in Surface Physics*, edited by R. Feder (World Scientific, Singapore, 1985).
[14] J. Kirschner, *Polarized Electrons at Surfaces* (Springer-Verlag, Berlin, 1985); S. F. Alvarado, R. Feder, H. Hopster, F. Ciccacci, and H. Pleyer, Z. Phys. B **49**, 129 (1982).
[15] K. v. Klitzing, G. Dorda, and M. Pepper, Phys. Rev. Lett. **45**, 494 (1980).
[16] Y. Xu, I. Miotkowski, C. Liu, J. Tian, H. Nam, N. Alidoust, J. Hu, C.-K. Shih, M. Zahid Hasan, and Y. P. Chen, Nat. Phys. **10**, 956 (2014).
[17] M. König, S. Wiedmann, C. Brüne, A. Roth, H. Buhmann, L. W. Molenkamp, X.-L. Qi, and S.-C. Zhang, Science **318**, 766 (2007).
[18] S. Murakami, N. Nagaosa, and S.-C. Zhang, Phys. Rev. Lett. **93**, 156804 (2004).
[19] J. E. Moore, Nature (London) **464**, 194 (2010).
[20] M. Z. Hasan and C. L. Kane, Rev. Mod. Phys. **82**, 3045 (2010).
[21] A. K. Geim and K. S. Novoselov, Nat. Mater. **6**, 183 (2007).
[22] S. A. Wolf1, D. D. Awschalom, R. A. Buhrman, J. M. Daughton, S. von Molnár, M. L. Roukes, A. Y. Chtchelkanova, and D. M. Treger, Science **294**, 1488 (2001).
[23] J. Kessler, *Polarized Electrons* (Springer-Verlag, Berlin, 1976).
[24] H. Hopster, D. L. Abraham, and D. P. Pappas, J. Appl. Phys. **64**, 5927 (1988).
[25] B. Leuer, G. Baum, L. Grau, R. Niemeyer, W. Raith, and M. Tondera, Z. Phys. D **33**, 39 (1995).
[26] S. N. Samarin, O. M. Artamonov, D. K. Waterhouse, J. Kirschner, A. Morozov, and J. F. Williams, Rev. Sci. Instrum. **74**, 1274 (2003).
[27] D. T. Pierce, R. J. Celotta, G.-C. Wang, W. N. Unertl, A. Galejs, C. E. Kuyatt, and S. R. Mielczarek, Rev. Sci. Instrum. **51**, 478 (1980).
[28] Kh. Zakeri, T. R. F. Peixoto, Y. Zhang, J. Prokop, and J. Kirschner, Surf. Sci. **604**, L1 (2010).
[29] R. Cortenraada, S. N. Ermolov, V. N. Semenov, A. W. Denier van der Gon, V. G. Glebovsky, S. I. Bozhko, and H. H. Brongersma, J. Cryst. Growth **222**, 154 (2001).
[30] S. Samarin, M. Tan, O. Artamonov, A. Baraban, P. Guagliardo, and J. Williams, J. Phys.: Conf. Series **601**, 012011 (2015).
[31] R. Feder, J. Phys. C: Solid State Phys. **14**, 2049 (1981).
[32] E. G. McRae and C. W. Caldwell, Jr., Surf. Sci. **2**, 509 (1964).
[33] S. Andersson, Surf. Sci. **19**, 21 (1970).
[34] U. Burgbacher, J. Braun, A. K. Brüning, A. B. Schmidt, and M. Donath, Phys. Rev. B **87**, 195411 (2013).
[35] P. Jennings and R. Jones, Adv. Phys. **37**, 341 (1988).
[36] N. D. Lang and W. Kohn, Phys. Rev. B **7**, 3541 (1973).
[37] G. Malmström and J. Rundgren, J. Phys. C **13**, L61 (1980).
[38] M. Nekovee, S. Crampin, and J. E. Inglesfield, Phys. Rev. Lett. **70**, 3099 (1993).
[39] M. Nekovee and J. E. Inglesfield, Prog. Surf. Sci. **50**, 149 (1995).
[40] F. Passek, M. Donath, K. Ertl, and V. Dose, Phys. Rev. Lett. **75**, 2746 (1995).
[41] J. Braun, C. Math, A. Postnikov, and M. Donath, Phys. Rev. B **65**, 184412 (2002).
[42] R. Jones and P. Jennings, Surf. Sci. Rep. **9**, 165 (1988).
[43] J. B. Pendry, *Low Energy Electron Diffraction* (Academic Press, New York, 1974).
[44] G. Malmström and J. Rundgren, Comput. Phys. Commun. **19**, 263 (1980).